Engineering Notes

ENGINEERING NOTES are short manuscripts describing new developments or important results of a preliminary nature. These Notes cannot exceed 6 manuscript pages and 3 figures; a page of text may be substituted for a figure and vice versa. After informal review by the editors, they may be published within a few months of the date of receipt. Style requirements are the same as for regular contributions (see inside back cover).

Graded Thermal Barrier—A New Approach for Turbine Engine Cooling

J. R. CAVANAGH,* K. R. CROSS,† R. L. NEWMAN,‡ AND W. C. SPICER†
Detroit Diesel Allison Division, General Motors Corporation, Indianapolis, Ind.

Background

A THERMAL barrier is a ceramic high temperature, low thermal conductivity structure, applied to turbine engine components to reduce the heat flux from hot gases. Engine performance is improved because of a reduction in the cooling air requirements.

Two approaches were pursued. The first, reported previously,[1] was Hastelloy-X honeycomb filled with ceramic and oversprayed with a dense ceramic coating. Both high and low density ceramics were studied. The second approach, described here, is a nonreinforced plasma sprayed coating where the composition is graded from 100% metal to 100% ceramic. The thermal shock test, used to evaluate the material, has been described elsewhere.[2] This test can be easily related to the thermal environment in an actual engine.

Material Development

Effectiveness of the thermal barrier increases as coating thickness increases; however, the thermal shock resistance decreases. The decrease in thermal shock resistance manifests in two distinct failure modes, 1) cracking in the outer surface of the ceramic phase or 2) separation of the ceramic coating from the substrate material. These facts have prevented widespread acceptance of plasma sprayed insulating coatings in the past. The approach chosen for minimizing these problems was the graded thermal barrier.

In practice, the graded thermal barrier has been applied as a five to six layer coating (up to 0.082 in. thick), starting with pure metal or alloy arc-plasma-sprayed on the Hastelloy X substrate and grading to pure ZrO_2 in the outer layer. The metal used was a nickel based alloy. The ceramic phase was ZrO_2, chosen primarily for its high melting (4600°F) point and low thermal conductivity.

Testing

The test criteria was summarized as follows: Thermal Shocks—able to survive thermal shocks at temperatures equivalent to 2500°F in an engine§, in a configuration similar to the intended use (burner liner or leading edge); Erosion—no erosion through coating for an exposure equivalent to 10 hours in a dusty engine environment; and Ballistic Impact—75% of thermal shock strength after impact. More details of the testing procedure are available in Refs. (1–3).

Results

The results of the primary screening test, thermal shock exposure, is summarized in Table I. A specimen representing today's state-of-the-art in uncooled monolithic Zirconia blades or vanes failed at 2400°F (and 40 shock cycles) by fracturing in two places. The surface was also marked by a mosaic crack pattern.[3]

The quantitative ballistic impact data relates the thermal shock resistance before and after the standard (¼ ft. lb.) impact. The graded thermal barrier specimens showed no degradation in thermal shock performance from ballistic trauma. Of special significance is the resistance of the burner liner specimen to large impact energy (1 ft. lb.) at normal incidence.

Discussion

The failure mechanism during thermal shock testing varied considerably with thickness and geometry as shown in Fig. 1 for the Ni-Cr-Mo based graded thermal barriers. It is clear

§ 2600°F for liner specimens, 3000°F for leading edge specimens.

Table I Median Test Results

Type of Material	Material	Thermal Shock Score[a] (Goal = 100) Burner Liner	Thermal Shock Score[a] (Goal = 100) Leading Edge	Erosion[b] (Goal = 10 hrs)	Ballistic Impact Source[c] (Goal = 75%)
Graded Coating	0.030 $NiAl/ZrO_2$	80	—	47.6 hrs.	East. 100%
	0.030 Ni–20 Cr/ZrO_2[d]	—	50	—	Est. 100%
	0.030 Ni–Cr–Mo/ZrO_2[d]	100M	40	12.4 hrs.	Est. 100%
Nongraded Coating	PS ZrO_2	—	—	59.5 hrs.	—
Monolithic Brick	ZrO_2 brick	—	40	308.6 hrs	Est. 100%
Dease-Reinforced[e]	HP/IHP ZrO_2	60	60	East 16.7 hrs.	70%
Foam-Reinforced[e]	Ceramic Foam	50	—	10 hrs.	66%

[a] Number of Thermal Shocks to Failure, Reference (2)
[b] Equivalent hours of dusty engine exposure (MIL-E-5007C
[c] Percent of Thermal Shock Score (based on flat specimens) retained after standard ballistic impact)
[d] Only specimens to pass tests
[e] From Reference (1)

Presented as AIAA Paper 72-361, at AIAA/ASME/SAE 13th Structures, Structural Dynamics, and Materials Conference, San Antonio, Texas, April 10–12, 1972; submitted April 12, 1972; revision received July 19, 1972.
Index categories: Structural Composite Materials (including Coatings); Thermal Modeling and Experimental Thermal Simulation.

* Engineering Technician.
† Senior Research Engineer.
‡ Senior Research Engineer. Member AIAA.

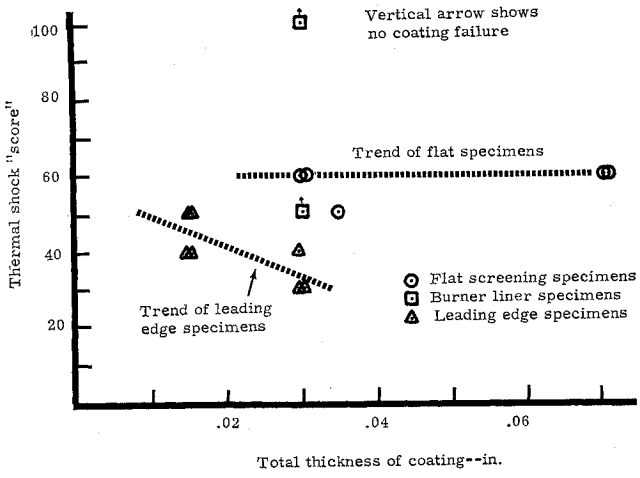

Fig. 1 Thermal shock score vs thickness—Hastelloy-X graded coatings.

from this figure that two mechanisms of failure are present. If thermal stress alone caused failure,[1] the thicker coatings would have a lower "score." This is not true for the flat specimens, all of which failed at the same point (and temperature level). Also the failure for these flat specimens was separation through a plane parallel to the surface. This seems to indicate reaction-caused degradation. The apparent failure mechanism was oxidation of the metal/ceramic composite just below the outer coating. The oxidation rate data support this supposition.[3]

During leading edge thermal shock testing some, but not all, of the specimens failed by cracking or blistering. If not caused by thermal stress, at least the thermal stress influenced the failure. The influence of thermal stress is made clear by the variation in thermal shock resistance with thickness (for a leading edge).

While thermal shock data are always suspect when geometries[4] are changed, it is of interest to compare our results with other literature values. Buckley[5] exposed thin coatings (0.009 to 0.024 in.) of ZrO_2 (flame and plasma sprayed) and of a $NiAl/ZrO_2$ composite (ungraded) to a plasma torch and recorded the number of cycles (heating and cooling) to failure. His results were—no failure¶ in flame sprayed ZrO_2 or composite coatings. The plasma sprayed ZrO_2 coatings failed at 3 cycles (0.009 in.) to 49 cycles (0.024 in.). The only direct comparison with our data is with the plasma sprayed coatings—his (0.015 in.) survived 30 cycles; ours (0.013 in.), 50. We found, contrary to Buckley, that thinner coatings exhibited greater shock resistance.

¶ In 50 shock cycles.

It would be instructive to have some basis for comparison between the several types of air cooling. This part describes the differences in cooling requirements for three types of cooling: simple convection, convection with a thermal barrier, and transpiration. Film cooling is beyond the scope of this paper and impingement can be considered a special case of convection.

In most preliminary design studies, it is customary to calculate cooling requirements based on a heat balance.[6] The heat absorbed by the cooling air is:

$$Q = \dot{m}_{cool} C_{P\,cool}(T_{cool_{out}} - T_{cool_{in}}) \quad (1)$$

The temperature rise of the cooling air, $(T_{cool_{out}} - T_{cool_{in}})$ is measured by the cooling effectiveness, η_c, where

$$\eta_c = (T_{cool_{out}} - T_{cool_{in}})/(T_{metal} - T_{cool_{in}}) \quad (2)$$

Typical values of η_c are 0.5 for convection and 0.9 for transpiration cooling.

However, for this analysis, we shall simply define our hot gas environment in terms of h_G. The heat transferred to the wall is

$$Q = h_G A(T_G - T_{metal}) \quad (3)$$

For both simple convection and transpiration, we will neglect the small temperature drop through the metal (or alternatively, use the exterior metal temperature to define η_c). We are also neglecting the blocking term in transpiration cooled structures. For structures protected by a thin ceramic insulation, of thickness δ_{TB} and conductivity K_{TB}, we use a reduced heat transfer coefficient, h^*,

$$h^* = \frac{1}{1/h_G + \delta TB/K_{TB}} \quad (4)$$

for flat plates. Figure 2 shows relationship between h^* and h_G for typical thermal barriers plotted as Q/Q_o vs h_G. This curve gives some idea of the relative help of thermal barriers—they are better the larger the h_G.

The only other term we need to balance the heat flows is T_M, the metal temperature. Typical, present day metals are limited to 1800°F for convection cooling and 1600°F for transpiration cooling. This is lower because of increased oxidation in the porous transpiration structure and the decreased strength caused by this structure.

Combining Eqs. (1), (2) and (4), we get

$$\frac{\dot{m}_{cool}}{A} = (h^*/C_{P\,cool}\,\eta c)[(T_G - T_{metal})(T_{metal} - T_{cool_{in}})] \quad (5)$$

Putting these in engine terms, high pressure ratio engines, with high compressor discharge temperature, favor convection cooling over transpiration cooling. High operating temperatures, with large values of $(T_G - T_M)$, favor transpiration cooling because of its large value of cooling effectiveness.

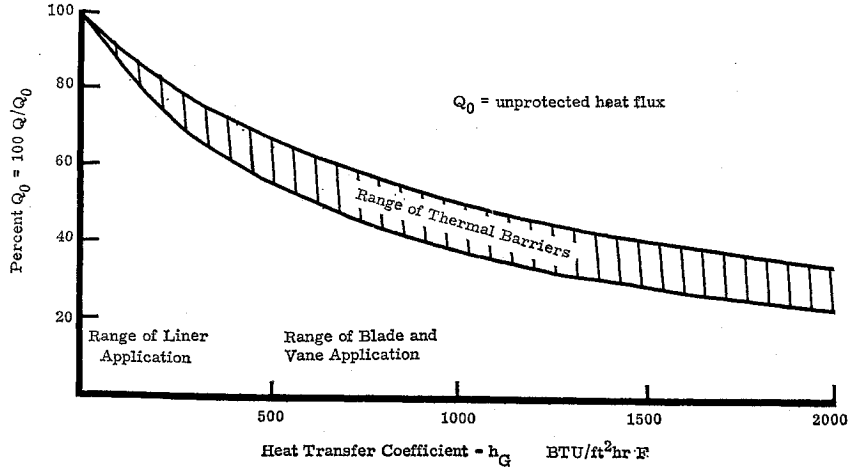

Fig. 2 Reduction of heat flux with a thermal barrier.

The thermal barrier, convection scheme will always use less air than the same no protection, convection scheme. How much more favorable depends "only" on the film coefficient. High pressure ratio engines with attendant high heat fluxes favor a thermal barrier approach.

References

[1] Newman, R. L., Cross, K. R., Spicer, W. C., Sheets, H. D. and Driskell, T. D., "Application of Thermal Barriers to High Temperature Engine Components," *Journal of Aircraft*, Vol. 9, No. 9, Sept. 1972), pp. 608–609.

[2] Spicer, W. C., Ross, P. T. and Newman, R. L., "A Well-Defined Thermal Shock Transient Test Burner," *Review of Scientific Instruments*, Vol. 43, No. 2, Feb. 1972, pp. 236–246.

[3] Cavanagh, J. R., Cross, K. R., Newman, R. L. and Spicer, W. C., "The Graded Thermal Barrier—A New Approach for Turbine Engine Cooling," AIAA Paper 72-361, San Antonio, Texas, April 1972.

[4] Newman, R. L., "Prediction of Thermal Shock Resistance During Very High Heating Rates," *Journal of American Ceramic Soc.*, Vol. 55, 1972, pp. 464–469.

[5] Buckley, J. D., "Thermal Conductivity and Thermal Shock Qualities of Zirconia Coatings on Thin Gage Ni-Mo-Cr Metal," *Bulletin of American Ceramic Society*, Vol. 49, No. 6, June 1970, pp. 588–591.

[6] Stepka, F. S., "Considerations of Turbine Cooling Systems for Mach 3 Flight," TN-D-4491, April 1968 NASA.

Selective Reinforcement of Wing Structure for Flutter Prevention

PAUL A. COOPER* AND W. JEFFERSON STROUD†
NASA Langley Research Center, Hampton, Va.

Introduction

THE anisotropic properties of filamentary composites permit a high degree of precision in tailoring and modifying stiffness and strength properties in a structure. This capability, coupled with the high strength and/or stiffness to weight ratio, make filamentary composite materials attractive for use in selectively reinforcing primary lifting surfaces of aircraft. This Note presents the results of an analytical study of the application of boron polyimide filamentary composite material to increase the flutter speed of a simple titanium full depth sandwich wing structure designed for strength. The sensitivity of the critical flutter speed to the location of patches of composite bonded to the skin of the wing is investigated.

Mathematical Model of Wing

The dimensions of the wing used in this study are shown in Fig. 1. The wing has a biconvex airfoil composed of variable thickness upper and lower cover plates which carry all the load; the wing is full of fuel. As in Ref. 1, plate theory is used in the structural analysis and piston theory is used in the flutter analysis, but with the structural analysis modified herein to take into account specially orthotropic (i.e., no direct coupling between bending and twisting, Ref. 2) filamentary composite layers on the wing covers, and with wing depth variation effects in the aerodynamic loading neglected.

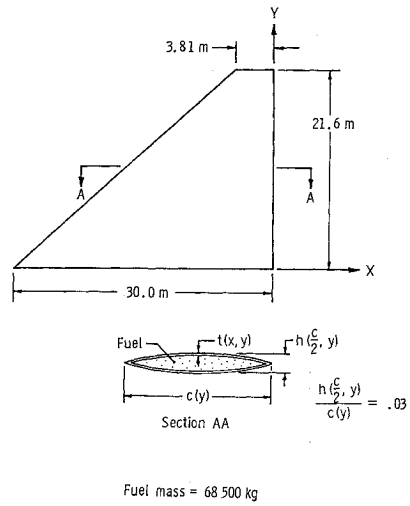

Fig. 1 Wing description.

All-Titanium Wings

Three all-titanium wings were designed to meet, respectively, flutter requirements only, strength requirements only, and both requirements. The wing is to a) be flutter-free at a velocity of 760 m/sec at an altitude of 7620 m ($M = 2.46$); b) support a uniformly distributed loading of 6900 N/m^2. The design process required determining four coefficients c_i in a polynomial representation of the thickness distribution of the wing cover plates

$$t = t_{\min} + \left[c_1\left(1-\frac{y}{y_S}\right) + c_2\left(1-\frac{y}{y_S}\right)^2\right]\left[1-\left(1-\frac{2x}{x_L}\right)\right] + \left[c_3\left(1-\frac{y}{y_S}\right) + c_4\left(1-\frac{y}{y_S}\right)^2\right]\left[1-\left(1-\frac{2x}{x_L}\right)\right] \times \left(1-\frac{2x}{x_L}\right) \quad (1)$$

in which $t_{\min} = 0.051$ cm, is the minimum gage requirement for all designs, x is the chordwise coordinate, y is the spanwise coordinate, x_L is the value of x at the leading edge, and y_S is the semispan. The thickness distribution described by Eq. (1) is minimum gage along the leading and trailing edges and at the tip. Mathematical programming techniques were used to determine values of the design variables c_i which give minimum weight and satisfy the flutter, strength, and minimum gage requirements.

Contour plots showing the cover plate thickness distributions for flutter strength, and combined strength-flutter designs are shown in Fig. 2 along with the mass, flutter speed, and ultimate load for each design. The flutter design meets the flutter requirement, but not the strength requirement. The strength design meets the strength requirement, but does not satisfy the flutter requirement. The strength-flutter design meets both requirements. All designs meet the minimum gage requirement. Because of the large mass of fuel (68,500 kg) carried in the wing, the contribution of the wing covers to the total mass distribution is small but is, nevertheless, included in the flutter analysis used to obtain these results. The primary effect of the thickness distribution is to establish the stiffness distribution.

Received April 14, 1972.
Index categories: Aircraft Structural Design; Structural Composite Materials; Optimal Structural Design.

* Aerospace Engineer, Design Studies Section, Structures Division. Associate Fellow AIAA.
† Aerospace Engineer, Automated Methods Section, Structures Division.